16-Electron Ruthenium(0) Complexes Containing the $Ru(NO)L_2^+$ Substructure: Planar $RuCH_3(NO)L_2$ vs Sawhorse $[Ru(NO)(C{=}C(SiMe_3)_2)L_2]^+$

Dejian Huang,[†] William E. Streib,[†] Odile Eisenstein,*[,‡] and Kenneth G. Caulton*[,†]

Department of Chemistry, Indiana University, Bloomington, Indiana 47405-7102, and LSDSMS (UMR 5636), Université de Montpellier 2, 34095 Montpellier Cedex 5, France

Received December 13, 1999

The synthesis and characterization of $RuCl(NO)L_2$ (L = P^iPr_3 and P^tBu_2Me) and $RuX(NO)L_2$ (X = F, CH_3, OSO_2CF_3, and H) are reported. All are planar at Ru. Reaction of $Ru(OSO_2CF_3)(NO)L_2$ with $NaBAr'_4$ (Ar′ = $C_6H_3(CF_3)_2$) in CH_2Cl_2 gives $RuCl(CH_2Cl)(NO)L_2^+$, while in C_6H_5F in the presence of $Me_3SiC{\equiv}CSiMe_3$, the vinylidene complex $Ru[C{=}C(SiMe_3)_2](NO)L_2^+$ is formed. The latter is a "sawhorse" structure (i.e., P's trans but NO and $C{=}C(SiMe_3)_2$ cis) and stands in contrast to the oxidative addition isomer $Ru(CO)(SiMe_3)(C{\equiv}CSiMe_3)L_2$ for the carbonyl analogue. The reason for the thermodynamic reversal for CO vs NO^+ is discussed on the basis of DFT/(B3PW91) calculations, and the calculated structure shows bending of the nitrosyl, consistent with considerable back-donation.

Introduction

We report here on synthetic access to the fragment $Ru(NO)L_2^+$, of zerovalent Ru, which allows evaluation of its reactivity, and (together with DFT (B3PW91) calculations) the relative thermodynamic stability of various isomeric products of its reaction with $Me_3SiC{\equiv}CSiMe_3$. Also accessible is $Ru(CH_3)(NO)L_2$, which stands as a comparison compound (pure σ donor CH_3 ligand) to previously reported[1,2] $Ru(CO)_2L_2$ and $Ru(CO)(NO)L_2^+$, whose nonplanar structures seem to contradict the conventional wisdom that four-coordinate d^8 species should be planar. The full characterization here of the vinylidene complex $Ru(NO)[CC(SiMe_3)_2]L_2^+$ reveals the influence of changing the π-acid ligand L′ in $Ru(EO)L'L_2$ (E = C or N^+). In particular, the inevitable question of bending of the M−N−O moiety must also be considered.

Changing ligands in a systematic manner better defines those factors that control the structure of four-coordinate d^8 species.

Experimental Section

General Comments. All reactions and manipulations were conducted using standard Schlenk and glovebox techniques. Solvents were dried and distilled under argon and stored in airtight solvent bulbs with Teflon closures. Most reagents are commercially available and degassed or dried before use. $RuCl_3(NO)(PPh_3)_2$[3] and $RuH_3Cl(P^tBu_2Me)_2$[4] were prepared according to the literature procedure. ^1H, ^{31}P, ^{19}F, and ^{13}C NMR were recorded on a Varian Gem XL300 or Unity I400 spectrometer. Chemical shifts are referenced to residual solvent peaks (^1H, ^{13}C), external H_3PO_4 (^{31}P), or $CFCl_3$ (^{19}F). Infrared spectra were recorded on a Nicolet 510P FT-IR spectrometer. Elemental analysis was performed on a Perkin-Elmer 2400 CHNS/O elemental analyzer at Indiana University. Purity of those compounds for which elemental analyses are not furnished due to thermolability or partial loss of volatile weak ligand or lattice solvent is to be ascertained from the spectra supplied as Supporting Information.

$RuCl(NO)(P^tBu_2Me)_2$. $RuH_3Cl(P^tBu_2Me)_2$ (200 mg, 0.44 mmol) was dissolved in diethyl ether (5 mL) and to the solution was slowly added isoamyl nitrite (55 μL, 0.44 mmol). The solution color immediately changed to green with gas evolution. The volatiles were evaporated to dryness, and the residue was washed with pentane and dried to give 0.17 g (80%) of green crystals. Anal. Calcd for $C_{18}H_{42}ClNOP_2Ru$: C, 44.40; H, 8.70; N, 2.87. Found: C, 44.84; H, 8.65; N, 3.38. ^1H NMR (C_6D_6, 400 MHz, 20 °C): 1.56 (vt, N = 5.6 Hz, 6H, PCH_3), 1.38 (vt, N = 12.8 Hz, 36H, $PC(CH_3)_3$). $^{31}P\{^1H\}$ NMR (162 MHz): 44.0 (br, s). IR (C_6D_6): 1707 (ν(NO)).

$RuF(NO)(P^tBu_2Me)_2$. $RuCl(NO)(P^tBu_2Me)_2$ (0.60 g, 1.23 mmol) and CsF (1.4 g, 9.0 mmol) were mixed in acetone (10 mL) and stirred at room temperature for 4 h to give a purple solution. The volatiles were evaporated, and the residue was extracted with pentane and filtered through a Celite pad. The filtrate was concentrated to ca. 5 mL and kept at −40 °C for 12 h. Dark purple crystals were formed, filtered, washed with pentane at −78 °C, and dried to yield 0.45 g (78%) of product. Anal. Calcd for $C_{18}H_{42}FNOP_2Ru$: C, 45.95; H, 9.00; N, 3.98. Found: C, 46.07; H, 8.68, N, 3.58. ^1H NMR (300 MHz, C_6D_6, 20 °C): 1.39 (vt, N = 13 Hz, 36H, $PC(CH_3)_3$), 1.30 (dvt, J = 2.4 Hz, N = 4.8 Hz, 6H, PCH_3). $^{31}P\{^1H\}$ NMR: 48.5 (d, J_{PF} = 38 Hz). ^{19}F NMR: −187 (t, J_{PF} = 36 Hz). IR (C_6D_6): 1703 (ν(NO)).

$Ru(OTf)(NO)(P^tBu_2Me)_2$. $RuF(NO)(P^tBu_2Me)_2$ (200 mg, 0.43 mmol) was dissolved in 10 mL of C_6H_6. Me_3SiOTf (78 μL, 0.43 mmol) was syringed into the solution, which immediately turned from purple to green. The mixture was stirred for 5 min, and the volatiles were evaporated to give a green solid,

* Corresponding author. E-mail: caulton@indiana.edu.
[†] Indiana University.
[‡] Université de Montpellier 2. E-mail: eisenst@lsd.univ-montp2.fr.

(1) Ogasawara, M.; Macgregor, S. A.; Streib, W. E.; Folting, K.; Eisenstein, O.; Caulton, K. G. *J. Am. Chem. Soc.* **1996**, *118*, 10189.
(2) Ogasawara, M.; Huang, D.; Streib, W. E.; Huffman, J. C.; Gallego-Planas, N.; Maseras, F.; Eisenstein, O.; Caulton, K. G. *J. Am. Chem. Soc.* **1997**, *119*, 8642.
(3) Fairy, M. B.; Irving, R. J. *J. Chem. Soc. (A)* **1966**, 475.
(4) Oliván, M.; Clot, E.; Eisenstein, O.; Caulton, K. G. *Organometallics* **1998**, *17*, 3091.

10.1021/om9909892 CCC: $19.00
Publication on Web 04/08/2000

which was recrystallized from toluene at −40 °C to give 0.15 g (58%) of dark green crystals. Anal. Calcd for $C_{19}H_{42}F_3NO_4P_2RuS$: C, 38.00; H, 7.05; N, 2.33. Found: C, 38.50; H, 7.02; N, 1.94. ^{1}H NMR (C_6D_6, 300 MHz, 20 °C): 1.68 (vt, N = 5.6 Hz, 6H, PCH_3), 1.28 (vt, N = 13.5 Hz, 36 H, $PC(CH_3)_3$). $^{31}P\{^1H\}$ NMR (20 °C, 121 MHz): 52.0 (s). ^{19}F NMR (282 MHz, 20 °C): −79.2 (CF_3SO_3). IR (C_6D_6): 1734 (ν(NO)).

[RuCl(CH_2Cl)(NO)(P^tBu_2Me)$_2$]BAr′$_4$. Ru(OTf)(NO)(P^tBu_2Me)$_2$ (100 mg, 0.17 mmol) and NaBAr′$_4$ (150 mg, 0.17 mmol) were mixed with CH_2Cl_2 (10 mL) and stirred at room temperature for 30 min to give a dark orange solution with precipitates. The mixture was centrifuged and the supernatant decanted to a flask and concentrated to ca. 3 mL. The solution was layered with pentane for 2 days to give dark orange crystals (144 mg, 61%). ^{1}H NMR (CD_2Cl_2, 400 MHz, 20 °C): 7.73 (s, 8H, *ortho*-H, of Ar′), 7.56 (s, 4H, *para*-H of Ar′), 5.96 (t, J_{PH} = 3.6 Hz, 2H, CH_2Cl), 1.67 (vt, N = 6.0 Hz, 6H, PCH_3), 1.46 (vt, N = 15 Hz, 36H, $PC(CH_3)_3$). $^{31}P\{^1H\}$ NMR (162 MHz, 20 °C): 38.1 (s). ^{19}F NMR (376 MHz, 20 °C): −62.0 (s, CF_3 of Ar′). IR (CD_2Cl_2): 1840 (ν(NO)).

[Ru(C=C($SiMe_3$)$_2$)(NO)(P^tBu_2Me)$_2$]BAr′$_4$. Ru(OTf)(NO)(P^tBu_2Me)$_2$ (100 mg, 0.17 mmol) and NaBAr′$_4$ (150 mg, 0.17 mmol) were mixed in fluorobenzene. To the mixture was syringed bis(trimethylsilyl)acetylene (40 μL, 0.18 mmol). The green color turned brown immediately. The mixture was stirred for 10 min and filtered through a Celite pad. The filtrate was evaporated to ca. 5 mL and layered with pentane for two weeks at − 20 °C to give dark orange crystals, which were filtered, washed with pentane, and dried in vacuo. Yield: 0.15 g (59%). ^{1}H NMR (400 MHz, 20 °C, in 9:1 (v/v) mixture of C_6H_5F and C_6D_{12}): 8.33 (s, 8H, *ortho*-H of Ar′), 7.80 (s, 4H, *para*-H of Ar′), 1.42 (vt, N = 5.7 Hz, 6H, PCH_3), 1.20 (vt, N = 13.5 Hz, 18H, $P(CH_3)_3$), 1.15 (vt, N = 14 Hz, 18H, $P(CH_3)_3$), 0.37 (s, 9H, $SiMe_3$), 0.30 (s, 9H, $SiMe_3$). The peaks at 0.37 and 0.30 ppm broaden and shift toward lower field as the temperature is raised and finally coalesce to a very broad peak centered at 0.37 ppm at 80 °C. At this temperature, the ^{t}Bu proton peaks (1.20 and 1.15 ppm) also coalesce to one broad peak at 1.25 ppm. $^{31}P\{^1H\}$ NMR: 48.2 (s). $^{13}C\{^1H\}$ NMR (C_6H_5F/C_6D_{12} = 9:1, 100 MHz, 20 °C): 284.1 (t, J_{PC} = 15 Hz, Ru=*C*), 100.9 (s, Ru=C=*C*), 38.1 (vt, N_{PC} = 18 Hz, P−CMe_3), 37.3 (vt, N = 20 Hz, P−CMe_3), 29.8 (s, $PC(CH_3)_3$), 28.6 (s, $PC(CH_3)_3$), 5.2 (vt, N_{PC} = 24.9 Hz, PCH_3), 2.75 (s, $SiMe_3$), 1.88 (s, $SiMe_3$). IR (C_6H_5F): 1642 (ν(NO)).

Ru(CH_3)(NO)(P^tBu_2Me)$_2$. RuF(NO)(P^tBu_2Me)$_2$ (100 mg, 0.21 mmol) was dissolved in pentane. To the solution was slowly added MeLi (1.4 mol/L, 150 μL). The solution color changed from purple to green with some precipitate. The mixture was centrifuged, and the liquid was decanted to a Schlenk flask, concentrated to ca. 3 mL, and cooled to −40 °C for 12 h. Dark green crystals were formed, filtered, washed with tetramethylsilane, and dried. Yield: 80 mg (82%). ^{1}H NMR (300 MHz, C_6D_6, 20 °C): 1.37 (vt, N = 12.4, 36H, $PC(CH_3)_3$), 1.32 (vt, N = 5.1, 6H, PCH_3), −1.7 (t, J = 9.7 Hz, 3H, Ru−CH_3). $^{13}C\{^1H\}$ NMR: 37.0 (vt, N = 15 Hz, PMe), 30.5 (s, $PCMe_3$), 9.54 (t, 15 Hz, Ru−CH_3). $^{31}P\{^1H\}$ NMR (121 MHz, C_6D_6, 20 °C): 48.4 (s). IR (C_6D_6): 1661 (ν(NO)). The preparation for the P^iPr_3 species proceeded analogously.

X-ray Structure Determination of Ru(CH_3)(NO)(P^iPr_3)$_2$. Crystals were grown from a toluene/pentane mixture. The crystals were mounted using silicone grease, and they were then transferred in a nitrogen stream to the goniostat, where they were cooled to −160 °C for characterization and data collection (Table 1). A preliminary search for peaks followed by analysis using programs DIRAX and TRACER revealed a primitive monoclinic cell. Following intensity data collection, the conditions $l = 2n$ for $h01$ and $k = 2n$ for $0k0$ uniquely determined space group $P2_1/c$. After an analytical correction for absorption (transmission factors 0.825−0.924), the structure was solved using the system DIRDIF-96, which revealed nearly the entire structure. The positions of the remaining non-hydrogen atoms were obtained from iterations of a least-squares refinement followed by a difference Fourier calculation. The ruthenium atom lies on a crystallographic center of symmetry; consequently the CH_3 and NO ligands are disordered, and the disorder places them very near one another. Nevertheless, they were resolved in the difference Fourier. Hydrogens were included for the ordered carbons in fixed, calculated positions with thermal parameters fixed at one plus the isotropic thermal parameter of the parent carbon. In the final cycles of refinement, the non-hydrogen atoms were varied with anisotropic thermal parameters, which, with a scale and extinction parameter, gave a total of 125 variables. The largest peak in the final difference map was a ruthenium residual of 0.89, and the deepest hole was −0.04 e/Å^3.

Table 1. Crystallographic Data for Ru(CH_3)(NO)(P^iPr_3)$_2$

formula	$C_{19}H_{45}NOP_2Ru$		
a, Å	7.994(1)	space group	$P2_1/c$
b, Å	8.946(1)	T, °C	−160
c, Å	16.605(2)	λ, Å	0.71069
β, Å	92.92(1)	ρ_{cald}, g/cm^{-3}	1.307
V, Å	1185.9(5)	μ(Mo Kα), cm^{-1}	8.0
Z	2	R	0.0283
fw	466.59	R_w	0.0319

[a] $R = \sum||F_o| - |F_c||/\sum|F_o|$. [b] $R_w = [\sum w(|F_o| - |F_c|)^2/\sum w|F_o|^2]^{1/2}$ where $w = 1/\sigma^2(|F_o|)$.

Ru($H)_3$(NO)(P^tBu_2Me)$_2$. Ru(CH_3)(NO)(P^tBu_2Me)$_2$ (10 mg, 0.021 mmol) was dissolved in C_6D_{14} (0.5 mL). The solution was degassed by freeze−pump−thaw cycles. H_2 (1 atm) was introduced, and the solution was warmed to room temperature. The green color gave way to pale yellow immediately. NMR analysis revealed clean formation of Ru($H)_3$(NO)(P^tBu_2Me)$_2$ and methane (0.22 ppm at −90 °C). ^{1}H NMR (300 MHz, −90 °C): 1.25 (br, 36H, $PC(CH_3)_3$), 1.12 (br, PCH_3), −4.26 (dt, J_{HH} = 7.3 Hz, 2H, Ru−H), −9.05 (tt, J_{PH} = 24.3 Hz, J_{HH} = 7 Hz, Ru−H). $^{31}P\{^1H\}$ NMR (121 MHz, −90 °C): 76.0 (s). IR (C_6D_6): 1676 (ν(NO)). This complex loses H_2 readily upon applying vacuum; therefore no attempts have been made to isolate it.

RuH(NO)(P^tBu_2Me)$_2$. Ru(CH_3)(NO)(P^tBu_2Me)$_2$ (10 mg, 0.02 mmol) was dissolved in cyclohexane (0.5 mL), degassed, and reacted with 1 atm H_2 at 25 °C to give immediately a pale yellow solution. The volatiles were removed, and the residue was subjected to vacuum for 30 min to give a dark brown solid, which was dissolved in C_7D_8 for spectral analysis. ^{1}H NMR (400 MHz): 1.49 (vt, N = 4.5 Hz, PCH_3), 1.18 (vt, N = 12 Hz, 36H, $PC(CH_3)_3$), −9.2 (t, J = 30 Hz, Ru−H). $^{31}P\{^1H\}$ NMR (162 MHz): 67.9 (s). IR (C_6D_6): 1658 (ν(NO)).

Computational Details

*C*alculations were carried out with the Gaussian 94[5] set of programs within the framework of DFT at the B3PW91 level.[6] The Hay−Wadt effective core potential (quasi-relativistic for the metal center) was used to replace the 28 innermost electrons of Ru[7] and the 10 core electrons of P and Si.[8] The associated double-ζ basis sets were used.[7,8] They were augmented by d polarization functions for P and Si.[9] H, C, O, and

(5) Frisch, M. J.; Trucks, G. W.; Schlegel, H. B.; Gill, P. M. W.; Johnson, B. G.; Robb, M. A.; Cheeseman, J. R.; Keith, T.; Petersson, G. A.; Montgomery, J. A.; Raghavachari, K.; Al-Laham, M. A.; Zakrzewski, V. G.; Ortiz, J. V.; Foresman, J. B.; Peng, C. Y.; Ayala, P. Y.; Chen, W.; Wong, M. W.; Andres, J. L.; Replogle, E. S.; Gomperts, R.; Martin, R. L.; Fox, D. J.; Binkley, J. S.; Defrees, D. J.; Baker, J.; Stewart, J. P.; Head-Dordon, M.; Gonzalez, C.; Pople, J. A. *Gaussian 94, Revision B3*; Gaussian, Inc.: Pittsburgh, 1995.
(6) Becke, A. D. *J. Chem. Phys.* **1993**, *98*, 5648.
(7) Hay, P. G.; Wadt, W. R. *J. Chem. Phys.* **1985**, *82*, 299.
(8) Wadt, W. R.; Hay, P. J. *J. Chem. Phys.* **1985**, *82*, 284.
(9) Höllwarth, A. H.; Böhme, M. B.; Dapprich, S.; Ehlers, A. W.; Gobbi, A.; Jonas, V.; Köhler, K. F.; Stegmann, R.; Veldkamp, A.; Frenking, G. *Chem. Phys. Lett.* **1993**, *208*, 237.

Scheme 1[a]

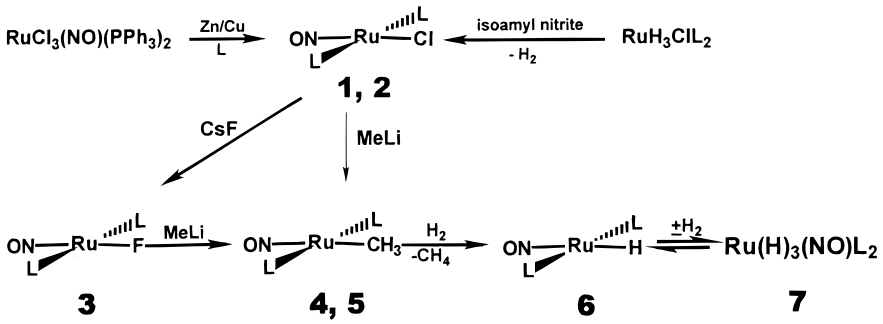

[a] **2**, **5** L = P^iPr_3; others L = P^tBu_2Me.

N were represented by a 6-31 G (d,p) basis set.[10] Full geometry optimization was performed without symmetry restriction.

Results

Synthesis of RuCl(NO)L$_2$. $RuCl(NO)L_2$ (**1**, L = P^tBu_2Me; **2**, L = P^iPr_3) can be synthesized by two routes: Reduction of $RuCl_3(NO)(PPh_3)_2$ by Zn/Cu alloy in hot benzene gives $RuCl(NO)(PPh_3)_2$, which undergoes phosphine exchange to give $RuCl(NO)L_2$ in moderate yield, a method that is highly dependent on the quality of Zn/Cu alloy.[11] More conveniently, **1** can be obtained quantitatively by the instantaneous reaction of RuH_3ClL_2 with equimolar isoamyl nitrite (Scheme 1). The reaction releases H_2, as is evidenced by evolution of gas. This is in agreement with the finding[11] that $RuCl(NO)(P^iPr_3)_2$ does not react with H_2. **2** was synthesized earlier from $RuCl_3(NO)(PPh_3)_2$ and reported[11] as "thermally unstable" and "can be stored only below −15 °C for a few days". In sharp contrast, we found that **1** and **2** are thermally stable up to 80 °C (in benzene) for more than 5 h, and the solid can be kept under argon atmosphere for months without any decomposition. The ^{1}H NMR spectrum of **1** shows only one *tert*-butyl proton resonance, consistent with a square-planar geometry similar to **2**, which was shown[11] by X-ray diffraction as having a linear NO. The NO stretching frequency of **1** (1707) is close to that of $RuCl(NO)(P^iPr_3)_2$ (1716 cm^{-1}).

RuF(NO)L$_2$. Stirring of **1** with excess CsF in acetone at room temperature (4 h, Scheme 1) gives $RuF(NO)L_2$, **3**, cleanly. Compound **3** is isolated as a purple solid, highly soluble in benzene, but less so in pentane. This represents a dramatic color change from the green chloride analogue. The ^{19}F NMR spectrum of **3** is a triplet at high field (−188 ppm) with relatively large J_{PF} (33 Hz). Correspondingly, the $^{31}P\{^1H\}$ NMR signal is a doublet with the same splitting. Similar to that of **1**, there is also only one virtual triplet for the ^{t}Bu protons, suggesting the phosphines are mutually trans, and the complex has a square-planar geometry with a linear NO. The ν_{NO} band at 1703 cm^{-1} is only slightly lower that that of the Cl complex, which is surprising since F is considered a much better π-donating ligand than chloride.[12] However, the strong electronegative character of F could contribute to a decrease of metal electron density, an effect that may be important for Ru(0). Compound **3** is also thermally stable up to 100 °C in toluene solution.

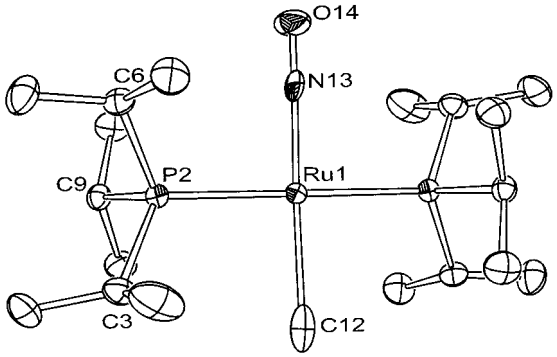

Figure 1. ORTEP diagram (30% probability ellipsoids) of $RuCH_3(NO)(P^iPr_3)_2$. Hydrogen atoms are omitted for clarity. Selected bond lengths: Ru1−P2 2.3827(8), Ru(1)−N(13) 1.823(12), Ru(1)−C(12) 2.293(16), O(14)−N(13) 1.059(16) Å. Selected bond angles: P(2)−Ru(1)−N(13) 90.2(3); P(2)−Ru(1)−C(12) 89.8(4); N(13)−Ru(1)−C(12) 170.9(7); Ru(1)−P(2)−C(3) 114.20(11); Ru(1)−P(2)−C(6) 113.28(9); Ru(1)−P(2)−C(9) 112.68(9)°; Ru(1)−N(13)−O(14) 177.3(10).

Ru(CH$_3$)(NO)L$_2$. Reaction of **1** and **2** with equimolar methyllithium (Scheme 1) gives clean formation of $RuMe(NO)L_2$, **4** and **5**, which are isolated as dark green crystals. The ^{1}H NMR spectrum of **4** also has one virtual triplet for the ^{t}Bu protons, in agreement with square-planar geometry. However, the Ru−CH_3 proton signal appears at unusually high field (−1.7 ppm) as a triplet (J_{PH} = 9.7 Hz). Although the high-field shift is usually an indication of agostic interactions, the normal $^1J_{CH}$ coupling value (127 Hz) in **4** suggests the opposite. We notice that the methyl (trans to NO) proton resonance of a saturated complex, $[Re(Me)(NO)(PMe_3)_4][C_5H_5]$, also appears at high field (−1.0 ppm).[13] Therefore, the high chemical shift may derive from CH_3 being trans to NO. The NO stretching frequency (1661 cm^{-1}) of **4** is significantly lower than that of **1** and **2**. Although methyl is not a π-donating ligand, the strong σ-donating ability of methyl strongly increases the electron density of the metal.

Crystal Structure of Ru(CH$_3$)(NO)(P^{i}Pr$_3$)$_2$, 5. While crystals of **4** suffer from severe disorder, $Ru(CH_3)(NO)(P^iPr_3)_2$ behaves somewhat better. X-ray quality crystals were grown from pentane at −40 °C, and the ORTEP diagram is depicted in Figure 1. The molecule has a crystallographic center of symmetry,

(10) Hariharan, P. C.; Pople, J. A. *Theor. Chim. Acta* **1973**, *28*, 213.
(11) Flügel, R.; Windmüller, B.; Gevert, O.; Werner, H. *Chem. Ber.* **1996**, *129*, 1007.
(12) Doherty, N. M.; Hoffman, N. W. *Chem. Rev.* **1991**, *91*, 553.
(13) Casey, C. P.; O'Connor, J. M.; Haller, K. J. *J. Am. Chem. Soc.* **1985**, *107*, 1241.

Scheme 2

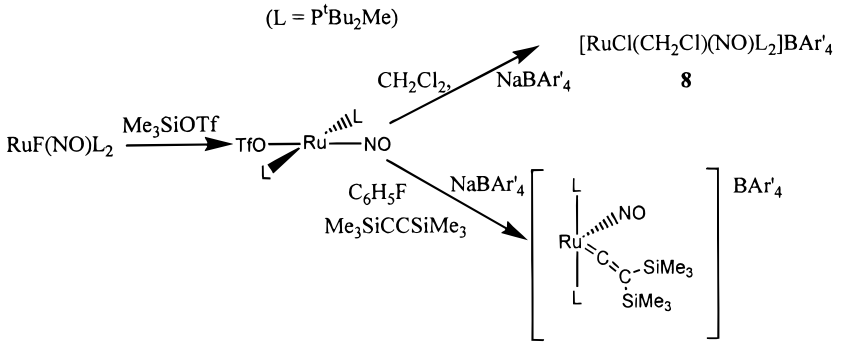

9

which gives 50/50 disorder of the CH_3 and NO ligands. The disorder could be modeled, but structural parameters must be interpreted with caution. The thermal parameters (Figure 1) of both N and C are longest along the bonds, a physically unreasonable result symptomatic of the close proximity of these atoms. The RuN distance (1.823(12) Å) is perhaps too long, compared to an average[14] of 1.74 Å, and the Ru−CH_3 distance (2.293 Å) is too long compared to an average[14] of 2.18 Å. Given these symptoms, the N−Ru−C angle (170.9(7)°) cannot confidently be said to deviate significantly (i.e., > 5°) from linearity.

$RuH(NO)L_2$ and $Ru(H)_3(NO)L_2$. $Ru(CH_3)(NO)L_2$ reacts with 1 equiv of H_2 at room temperature to give $RuH(NO)L_2$, **6** (Scheme 1). Monitoring the reaction at −80 °C does not give evidence for any possible primary products ($Ru(H_2)(CH_3)(NO)L_2$ or $Ru(H)_2(CH_3)(NO)L_2$); instead, only $Ru(H)_3(NO)L_2$ and CH_4 are observed along with $RuCH_3(NO)L_2$. If the reaction mixture is warmed to roomtemperature, $RuH(NO)L_2$ is formed and remaining $Ru(CH_3)(NO)L_2$ is consumed. This fact itself suggests that $RuH(NO)L_2$ reacts much faster with H_2 than does $Ru(CH_3)(NO)L_2$. The hydride of **6** appears at −9.00 ppm as a triplet, and there is also only one virtual triplet for the ^{t}Bu protons, in agreement with a square-planar geometry. The NO stretching frequency (1658 cm^{-1}) of **6** is close to that of **4**. Compound **6** stands as the first 16-electron Ru(0) hydride complex. The hydrides of $Ru(H)_3(NO)L_2$ appear as a broad peak at −6 ppm at 20 °C, indicating fast exchange among the three H and also some exchange with added free H_2, which appears as an extremely broad peak at room temperature. At −40 °C (in toluene-d_8), the free H_2 peak is sharp, suggesting slow exchange with the hydrides, while the hydride signals have just started to decoalesce. At lower temperature (−80 °C), the hydride signal decoalesces to two peaks with 2:1 ratio, at −4.3 ppm (2H) and −9.3 ppm (1H). The large but identical T_1 values (220 ms, −80 °C) of the two hydride signals suggest that **7** is a trihydride complex, with H exchange fast enough to average the T_1. Detailed hydride exchange dynamics and mechanism will be published in a separate paper, along with the chemistry of the Os analogue, $Os(H)_3(NO)L_2$.[15]

$Ru(OTf)(NO)L_2$. Reaction of $RuF(NO)L_2$ with 1 equiv of Me_3SiOTf (OTf = O_3SCF_3) in benzene (Scheme 2) gives clean formation of $Ru(OTf)(NO)L_2$. The dark green complex has a higher NO stretching frequency (1734 cm^{-1}) than that of $RuF(NO)L_2$, in agreement with weaker donating power of OTf. The presence of one ^{t}Bu ^{1}H NMR virtual triplet is in agreement with a planar geometry.

Replacement of OTf (Scheme 2). Salt metathesis between RuR(OTf)(CO)L_2 (L = P^{t}Bu$_2$Me, R = H, Ph, Me) and NaBAr′$_4$ has been shown to yield formally 14-electron Ru(II) complexes [RuR(CO)L_2]BAr′$_4$ with two agostic interactions.[16,17] Salt metathesis between Ru(OTf)(NO)L_2 and NaBAr′$_4$ would thus lead to [Ru(NO)L_2]BAr′$_4$. Reaction of equimolar NaBAr′$_4$ with Ru(OTf)(NO)L_2 in CH_2Cl_2 results in an immediate color change from green to dark orange. After workup, dark orange crystals (**8**) are obtained in good yield. ^{1}H NMR analysis of product reveals a triplet at 6.0 ppm (J_{PH} = 3.6 Hz) with integration of two protons for an Ru−CH_2Cl functionality. There are also two virtual triplets for ^{t}Bu protons, indicating diastereotopic ^{t}Bu groups. The NO stretching frequency is rather high (1840 cm^{-1}) in comparison with that of Ru(OTf)(NO)L_2 (1734 cm^{-1}), in agreement with a higher oxidation state of Ru. According to the geometry preference of five-coordinated Ru(II) complexes, we conclude that a CH_2Cl group occupies the site trans to the vacant site and Cl is trans to NO, favoring push−pull stabilization. The fact that this reaction gives H_2ClC−Cl oxidative addition (cf. RuH(CO)L_2(η^2-Cl_2CH_2)$^+$ for a Ru(II) reagent[16,17]) supports the idea that $Ru(NO)L_2^+$ is still a reducing species, despite the strong π-acid nitrosyl ligand.

Four-Coordinate Ru(0) Vinylidene. Combination of equimolar Ru(OTf)(NO)L_2, NaBAr′$_4$, and Me_3SiCC-$SiMe_3$ in fluorobenzene immediately results in a deep brown solution with a fine precipitate (Scheme 2). After centrifuging and layering of the liquid with pentane for 2 days, deep brown crystals were obtained. Spectroscopic analysis of the crystals support a vinylidene complex, [Ru(C=C(SiMe$_3$)$_2$)(NO)L_2]BAr′$_4$, **9**. The ^{13}C-{^{1}H} NMR spectrum gives a triplet at 284 ppm (J_{PC} = 15 Hz) and a singlet at 101 ppm for the α- and β-carbon of vinylidene. Two sets of ^{13}C NMR peaks are also found for diastereotopic ^{t}Bu primary and tertiary carbons, and two singlets at 2.7 and 1.9 ppm are assigned to the carbons of two $SiMe_3$ groups. Inequivalent ^{t}Bu groups

(14) Orpen, A. G.; Brammer, L.; Allen, F. H.; Kennard, O.; Watson, D. G.; Taylor, R. *J. Chem. Soc., Dalton Trans.* **1989**, S1.
(15) Yandulov, D.; Caulton, K. G. *Inorg. Chem.*, in press.
(16) Huang, D.; Streib, W. E.; Eisenstein, O.; Caulton, K. G. *Angew. Chem., Int. Ed. Engl.* **1997**, *36*, 2004.
(17) Huang, D.; Huffman, J. C.; Bollinger, J. C.; Eisenstein, O.; Caulton, K. G. *J. Am. Chem. Soc.* **1997**, *119*, 7398.

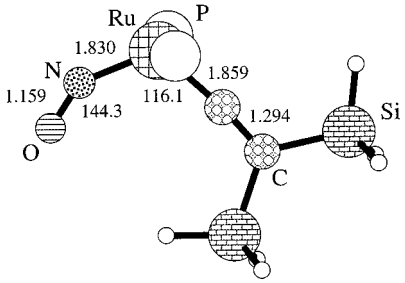

Figure 2. Optimized (B3PW91) structure (distances in Å, angles in deg) for $Ru(NO)(C{=}C(SiH_3)_2)(PH_3)_2^+$. Hydrogens of PH_3 have been removed for clarity.

demand that the Ru coordination geometry is nonplanar. Consistently, two ^1H NMR virtual triplets and two singlets are found for the ^{t}Bu and $SiMe_3$ groups, respectively. Inequivalent $SiMe_3$ groups require that the vinylidene plane be perpendicular to the P−Ru−P axis and the $C(SiMe_3)_2$ group rotates only slowly on ^1H NMR time scale. The NO stretching frequency of **9** is low (1642 cm^{-1}) in comparison with that of $[Ru(NO)(CO)L_2]^+$ (1709 cm^{-1}), indicating more back-donation from Ru to NO in the former. On the basis of these data we propose the complex has a nonplanar geometry with two phosphines trans to each other and with N and the vinylidene C_α bending toward each other. Two X-ray data sets both indicated the crystals to be twinned. DFT (B3PW91) optimization of $Ru(CC(SiH_3)_2)(NO)(PH_3)_2^+$ gives a sawhorse structure (Figure 2) with an N−Ru−C angle equal to 116°. The $NRuC_\alpha$ and $C_\beta Si_2$ units are coplanar, and the NO ligand is significantly bent (Ru−N−O = 144.3°) with O toward the vinylidene ligand. The PH_3 ligands are trans to each other, although the P−Ru−P angle deviates from linearity (165.5°). This structure, which fully agrees with the experimental data, emphasizes the role of the π-acceptor ligands in the preference for a sawhorse geometry. The vinylidene orientation permits the empty p carbenoid orbital to overlap with $d_{x^2-y^2}$. (**10**). Strong electron transfer into

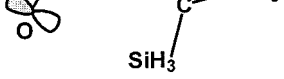

10

π^*_{NO} has also occurred, as shown by the RuNO angle. The angle between the two cis acceptor ligands decreases with their π-accepting capability. Thus, in the isoelectronic $Ru(CO)(CC(SiH_3)_2)(PH_3)_2$ structure, the C−Ru−C angle is calculated to be 130.7°, which is larger than with NO (116.0°). The sawhorse structure of this vinylidene complex is in agreement with that of other d^8 ML_4 complexes bearing several π-acceptor ligands.[1,2]

The nonplanar nature of $Ru(CO)_2(P^tBu_2Me)_2$ and $[Ru(NO)(CO)L_2]^+$ suggests that inversion at Ru could control their fluxional behavior. The difference in energy between the sawhorse and planar structure of $Ru(NO)(CO)(PH_3)_2^+$ is calculated to be 13.3 kcal/mol, and the estimated experimental value of $Ru(NO)(CO)(P^tBu_2Me)_2^+$ is higher (19.1 kcal/mol, at 100 °C), as it includes effects of ion pairing and steric bulkiness of the phosphine ligand.[2] The two Me_3Si proton singlets and the two ^{t}Bu virtual triplets of $[Ru(NO)(C{=}C(SiMe_3)_2)L_2]^+$ coalesce to baseline at around 80 °C in fluorobenzene, which permits evaluation of the barrier for Me_3Si group exchange as 13.3(4) kcal/mol (at 80 °C) and that of ^{t}Bu exchange as 13.5(4) kcal/mol. Since these are identical, a single process effects both site exchanges. We propose that this process is going to a planar geometry around Ru (eq 1). While $Ru{=}C{=}C(SiMe_3)_2$ rotation itself can

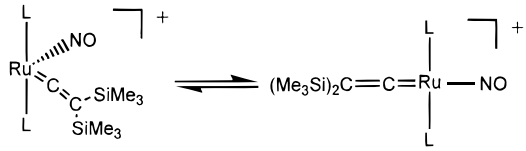

(1)

interconvert the Me_3Si groups, it does not average the ^{t}Bu signals, so this rotation alone is not sufficient to explain the behavior of $Ru[CC(SiMe_3)_2](NO)L_2^+$. This hypothesis is preferred, although rotational barriers of vinylidene ligands have been found experimentally to be in the range from 7 to 12 kcal·mol^{-1},[18] with a few exceptions, like $[(\eta^5\text{-}C_5H_5)Re(NO)(PPh_3)(CCRR')]^+$, where the barrier was found to be around 20 kcal·mol^{-1}.[19]

Thermodynamics of Reactions of $Ru(NO)L_2^+$ vs $Ru(CO)L_2$. The products of $Ru(CO)L_2$ and $Me_3SiC{\equiv}CSiMe_3$ appear to have a ground-state structure,[20] where oxidative addition of the Si−C(sp) bond has occurred to give a square-pyramidal Ru(II) product, **11**.

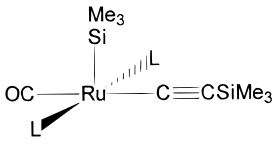

11

To understand these differences, we have calculated the products of reaction of HCCH and $H_3Si{-}CC{-}SiH_3$ with $Ru(NO)(PH_3)_2^+$ and $Ru(CO)(PH_3)_2$. Three types of products were considered: the alkyne adduct, the vinylidene product, and the product resulting from the oxidative addition of the metal to the C−H or C−Si bonds. The energies relative to the most stable isomer within each group are given in Table 2.

The results show an important dependence of the relative stabilities of the products with the nature of the ancillary ligand (CO or NO^+) and the alkyne substituent. For HCCH, the vinylidene product is the most stable and the alkyne adduct is significantly higher in energy (6−7 kcal·mol^{-1}) for both CO and NO ancillary ligands. The products of oxidative addition are far above in energy for NO (16.2 kcal·mol^{-1}) but almost isoenergetic to the vinylidene complex for CO (0.7 kcal·mol^{-1}).

(18) (a) Consiglio, G.; Bangerter, F.; Darpin, C.; Morandini, F.; Lucchini, V. *Organometallics* **1984**, *3*, 1446. (b) Consiglio, G.; Morandini, F. *Inorg. Chim. Acta* **1987**, *127*, 79. (c) Boland-Lussier, B. E.; Churchill, M. R.; Hughes, R. P.; Rheingold, A. L. *Organometallics* **1982**, *1*, 628. (d) Gamasa, M. P.; Gimeno, J.; Lastra, E.; Martin, B. M.; Anillo, A.; Tiripicchio, A. *Organometallics* **1992**, *11*, 1373. (e) Beddoes, R. L.; Bitcon, C.; Grime, R. W.; Ricalton, A.; Whiteley, M. W. *J. Chem. Soc., Dalton Trans.* **1995**, 2873.

(19) Senn, D. R.; Wong, A.; Patton, A. T.; Marsi, M.; Strouse, C. E.; Gladysz, J. A. *J. Am. Chem. Soc.* **1988**, *110*, 6096

(20) Huang, D.; Heyn, R. H.; Bollinger, J. C.; Caulton, K. G. *Organometallics* **1997**, *16*, 292.

Table 2. DFT Energies (kcal·mol^{-1}) of Products of RuL′$(PH_3)_2^+$ and RCCR, R = H or SiH_3[a]

ligand	L′ = NO^+	L′ = CO
CCH_2	0	0
HCCH	6.8	6.0
(H)/(CCH)	16.2	0.7
$CC(SiH_3)_2$	0	11.5
$H_3SiCCSiH_3$	2.5	11.2
$(SiH_3)/CCSiH_3$	6.1	0

[a] The alkyne adducts have a square-planar structure with the alkynes perpendicular to the molecular plane. The (H)/(CCH) and $(SiH_3)/(CCSiH_3)$ have a square-pyramidal geometry with H or SiH_3 at the apical site.

Going to disilylacetylene decreases the difference in energy between the vinylidene complex and the alkyne adduct. However, the most remarkable change concerns the relative energy of the oxidative addition product. $Ru(NO)(SiH_3)(CCSiH_3)(PH_3)_2^+$ is the least stable isomeric product of its group, whereas $Ru(CO)(SiH_3)(CCSiH_3)(PH_3)_2$ is the most stable isomeric product of its group. This reversal was already developing in the HCCH family but has been greatly enhanced by the presence of the silyl groups.

These results are in good agreement with the experimental observations in the case of disilylalkynes. The preference for a vinylidene isomer over the η^2-alkyne adduct in the case of NO will contain additional steric factors for $SiMe_3$ (vs SiH_3, Table 2) due to the closer proximity of the silyl to the phosphine ligands in the η^2-alkyne adduct.

The remarkable change in products upon the change of a good π-acceptor ligand (CO) by an even better one is certainly surprising, and the calculations indicate that this change could also happen for other alkynes.

The calculations reported here also permit some conclusions regarding substituent effects (the H/SiH_3 transposition) on the η^2-alkyne, vinylidene, and oxidative addition isomers:

(1) The alkyne competition reaction is essentially thermoneutral:

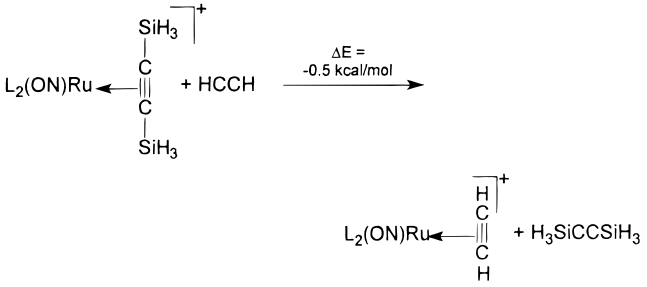

(2) The competition among oxidative addition products favors H−C and Si−Ru bonds over Si−C and H−Ru bonds:

$$Ru(SiH_3)(C{\equiv}CSiH_3)(NO)L_2^+ + HCCH \xrightarrow[=+5.2\ \text{kcal/mol}]{\Delta E} RuH(C{\equiv}CH)(NO)L_2^+ + H_3SiCCSiH_3$$

This is consistent with SiR_3 being a potent electron donor to electron-deficient Ru.

(3) The competition among vinylidene products favors H on the coordinated vinylidene and Si on the free alkyne:

$$Ru(NO)(C{=}CH_2)L_2^+ + H_3SiCCSiH_3 \xrightarrow[=+4.9\ \text{kcal/mol}]{\Delta E} Ru(NO)(C{=}C(SiH_3)_2)L_2^+ + HCCH$$

All three of these trends also hold for the $Ru(CO)L_2$ analogues.

Conclusions

The present synthetic sequence M−Cl → M−F → M−OSO_2CF_3 → M^+ has been effective in several recent instances of production of high unsaturation. The first step depends on mass action (excess CsF); the second, on the strength of the Si−F bond produced. The last step is a tribute to the high Lewis acidity of sodium in anhydrous $NaBAr'_4$ when used in a noncoordinating solvent (here C_6H_5F) and where the product NaO_3SCF_3 is presumably insoluble. Since no bond is formed to M^+, and charge separation is also required, it is necessary that the M−OSO_2CF_3 bond dissociation energy be small for this synthetic strategy to succeed.

The fact that the 14-electron fragment $Ru(NO)L_2^+$ oxidatively adds the C−Cl bond of CH_2Cl_2 and isomerizes $Me_3SiC{\equiv}CSiMe_3$ to the vinylidene $C{=}C(SiMe_3)_2$ is consistent with this metal center being more reducing (π-basic) than electron-deficient (14 valence electrons). In particular, an η^2-alkyne is probably less electron-withdrawing/oxidizing than either full oxidative addition of the Si−C bond or the vinylidene ligand. However, the less electron-withdrawing CO permits "full" oxidative addition (**11**) in a way that the NO^+ analogue does not.

DFT calculations show a determining influence of the ancillary ligand and alkyne substituents on the products of reaction. This is due to the fact that the possible isomeric structures are reasonably close in energy. This permits reversal of products to occur by even subtle change in the nature of reactants.

Acknowledgment. This work was supported by the ACS-PRF, the University of Montpellier 2, and the French CNRS.

Supporting Information Available: Crystallographic details for $Ru(CH_3)(NO)(P^iPr_3)_2$. Also available are NMR spectra for five compounds. This material is available free of charge via the Internet at http://pubs.acs.org.

OM9909892